Supplementary Information

Generation of binder-format-payload conjugate-matrices by antibody chain-exchange

Vedran Vasic[1&], Steffen Dickopf[1,2&], Nadine Spranger[1,3], Rose-Sophie Rosenberger[1], Michaela Fischer[1], Klaus Mayer[1], Vincent Larraillet[1], Jack A. Bates[1], Verena Maier[1], Tatjana Sela[1], Bianca Nussbaum[1], Harald Dürr[1], Stefan Dengl[1] & Ulrich Brinkmann[1*]

1 Roche Pharma Research and Early Development (pRED), Large Molecule Research (LMR), Roche Innovation Center Munich, Penzberg, Germany

2 current affiliation: Veraxa Biotech, Heidelberg, Germany

3 current affiliation: Institute of Molecular Immunology, School of Medicine and Health, Technical University Munich (TUM), Munich, Germany

& VV and SD are equal contributors

* to whom correspondence should be addressed: ulrich.brinkmann@roche.com

Supplementary Figures

Supplementary Fig. 1: Production and characterization of Fc donor and binder-acceptor molecules

Binder-acceptor molecules: Antibody derivatives that bind HER2 or EGFR were expressed in transiently transfected HEK293 cells using the Expi293 expression system (Thermo Fisher Scientific). Antibody derivatives were purified from the supernatant by protein A affinity chromatography and subsequent SEC. Each binder was produced in three different formats, with the Fab region located either N-terminal to the Fc, C-terminal to the Fc, or both. Heterodimerization of Fc heavy chains was directed via knob-into-hole mutations in the CH3 domains[1] (see Methods section), with the hole mutations located on the heavy chain containing the binder (referred to as the productive chain). In a complementary manner, the knob mutation was located on the dummy chain. The destabilizing mutation K370E was included in the CH3 domain of the dummy knob chain, as in ref (2). To remove by-products after chain exchange, the dummy chain harbors a C-terminal C-Tag, a four-amino acid affinity tag (EPEA, Supplementary Fig. 1a). The C-tag allows by-products, unreacted educts, and aggregates to be removed using a CaptureSelect C-tagXL affinity column (Thermo Fisher Scientific). Exemplary non-reducing and reducing SDS-PAGE (Supplementary Fig. 1b) and SEC profiles (Supplementary Fig. 1c) reveal the homogeneity and correct composition of purified binder educts. With the exception of the Cetuximab N+C format, which had a relatively low yield, expression yields ranged between 50 and 150 mg/L, with 90-99% purity achieved without process optimization.

Fc-donor molecules for subsequent conjugation: The Fc donor molecules also carry knob-into-hole mutations in their CH3 interface to promote heterodimerization, and charge mutations that result in partial destabilization of the CH3 heterodimer to drive the chain-exchange reaction. Complementary to the binder educts, which contain hole mutations in the CH3 domain of the productive chain, the Fc donor molecules contain a knob mutation in the productive chain, which transfers the payload to the binder acceptor educt. The dummy chain contains hole mutations as well as the destabilizing interface mutation E357K in the CH3 domain[2]. The dummy chain also contains a C-terminal C-tag. Some Fc donor molecules harbor a Q-Tag (YRYRQ) on the productive heavy chain to enable site-specific payload conjugation with a microbial transglutaminase (MTG), as described in detail in Supplementary Fig. 5. Three different Fc donor precursors formats were produced, which differ in the position and number of Q-Tags present (Supplementary Fig. 1d). Two of the formats have only one Q-Tag either at position 221 or 297. One Fc donor precursor harbors a Q-Tag at both positions (221 and 297). Analogous to the binder acceptor molecules, all Fc donor molecules were produced by transient expression using the Expi293 expression system (Thermo Fisher Scientific). Expression yields greater than 40 mg/L were achieved. SDS-PAGE and analytical SEC was performed to characterize the molecules - shown here exemplarily for Fc(Q-Tag_221). The presence of the intact Fc donor precursor was confirmed by a strong band at 50 kDa in non-reducing SDS-PAGE, and as bands of approximately 27 kDa in reducing SDS-PAGE, which correspond to the productive and dummy Fc chains (Supplementary Fig. 1e). Analytical SEC (Supplementary Fig. 1f) shows a purity greater than 90%.

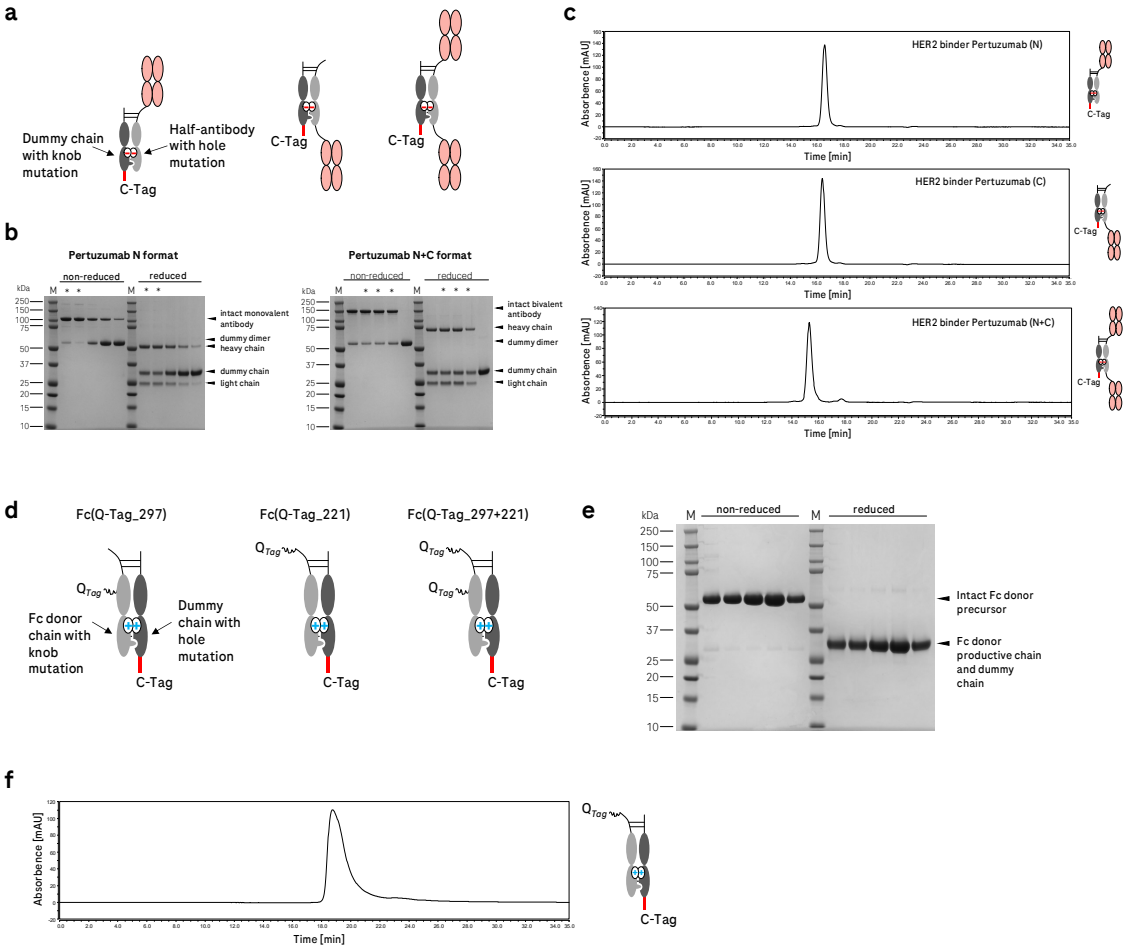

Supplementary Fig. 1: Production and characterization of Fc donor and binder-acceptor molecules. a Illustration of binder-acceptor molecules in the N-terminal (left), C-terminal (middle), and N+C-terminal format (right). **b** Exemplary Coomassie SDS-PAGE analysis of fractions after SEC purification of a Pertuzumab N-format acceptor molecule (left) and a Pertuzumab N+C acceptor molecule (right). *The fractions selected for pooling are indicated with asterisks. M: molecular weight marker. This experiment was performed one time. **c** Analytical SEC chromatograms of purified Pertuzumab-derived acceptor modules in the N- (top), C- (middle), and N+C-format (bottom). **d** Illustration of Fc donor molecules with three different Q-tag positions, as indicated. **e** Exemplary Coomassie SDS-PAGE analysis of SEC purification fractions of an Fc donor molecule with a Q-tag at position 221 (middle molecule from Supplementary Fig. 1d). All of the fractions analyzed in this gel were pooled. M: molecular weight marker. This experiment was performed one time. **f** Analytical SEC chromatogram of the Fc(Q-Tag_221) donor molecule from Supplementary Fig. 1e.

Supplementary Fig. 2: Chain-exchange-mediated attachment of horseradish peroxidase (HRP)

Conversion of randomly conjugated Fc donor molecules into defined antibody derivatives with unmodified binding regions can be achieved not only for small molecular weight payloads such as fluorescent dyes, but also for large molecules including enzymes. In Supplementary Fig. 2, an Fc donor molecule containing NHS-conjugated horseradish peroxidase (HRP) was combined in a pair-FORCE reaction with an EGFR-binding antibody acceptor molecule (clone C225)[3]. The combined functionalities of EGFR-binding and HRP enzyme activity were demonstrated by applying the pair-FORCE product as a Western blot detection reagent. The resulting anti-EGFR-HRP conjugate detects EGFR in total cell lysates of A431 cells with high specificity and low background. Thus, chain-exchange-mediated ADC generation is not only limited to the coupling of small molecular weight compounds, but is also applicable for large molecule payloads.

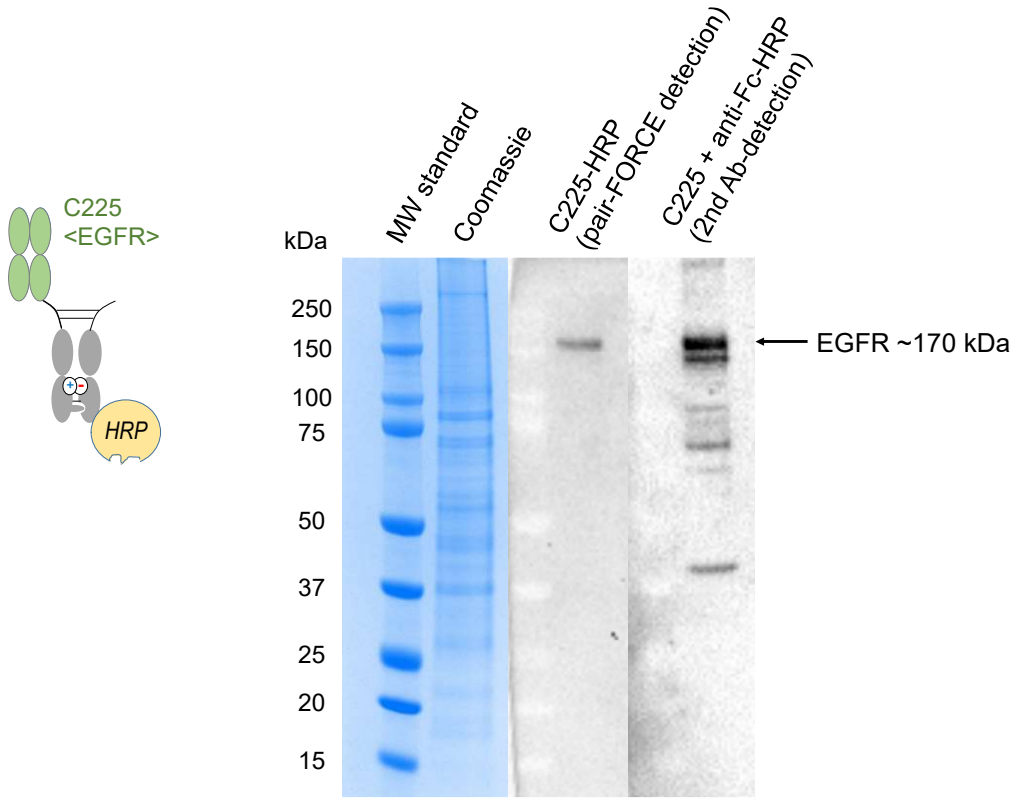

Supplementary Fig. 2: Chain-exchange-mediated attachment of HRP onto an EGFR-binding antibody derivative. Horseradish peroxidase (HRP) was attached via pair-FORCE to an EGFR-binding antibody acceptor molecule derived from clone C225[3]. A band corresponding to EGFR was observed in the Western blot of A431 total cell lysate, demonstrating the functionality of the binder to detect denatured EGFR, as well as HRP activity after pair-FORCE. To confirm the specificity of the C225-HRP pair FORCE conjugate, an unlabeled C225-derived anti-EGFR antibody was applied as the primary antibody, followed by blotting with an HRP-conjugated secondary antibody (anti-human Fc). MW standard: molecular weight standard. The experiment above was performed one time.

Supplementary Fig. 3: Application of pair-FORCE-generated EGFP-fusions for epitope binning

Antibody derivatives harboring EGFP can be generated by pair-FORCE to provide fluorescent fusion-protein derivatives of different antibodies in a simple and robust manner. A common application that requires sets of comparably labeled antibodies directed at the same antigen is epitope binning[4]. Exchange-generated antibody-EGFP fusions can therefore be applied for such assays, demonstrating the suitability of the pair-FORCE technology for epitope binning applications.

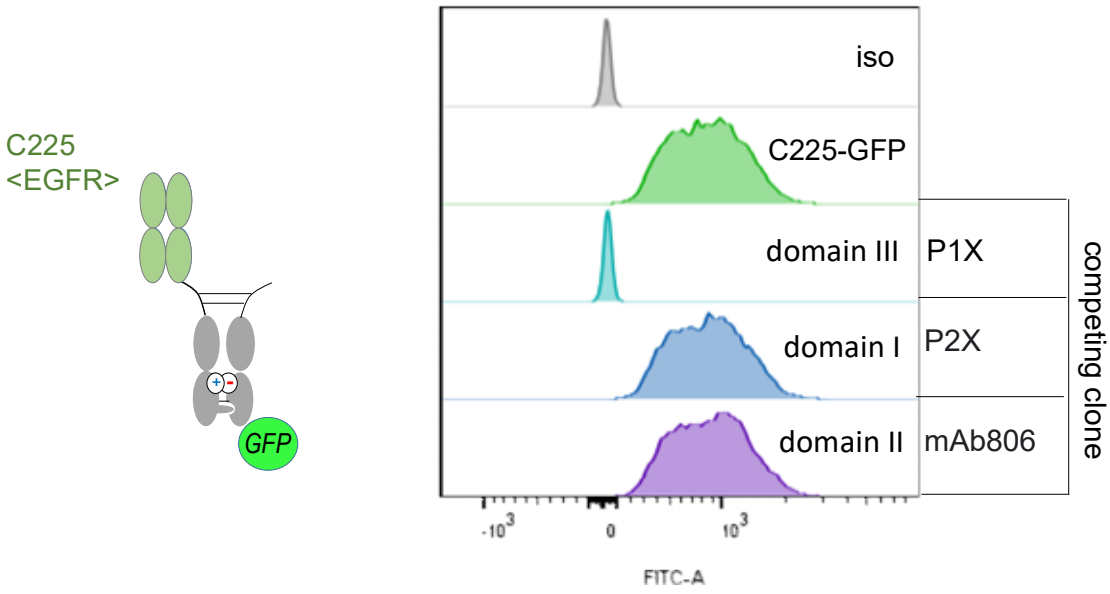

Supplementary Fig. 3: EGFR-binding, EGFP fusion proteins generated by pair-FORCE allow for epitope binning assays. An EGFR-binding acceptor molecule based on the C225 (Cetuximab) sequence[3] was subjected to chain-exchange with an Fc donor molecule containing an EGFP fusion protein at its C-terminus. Flow cytometry analysis demonstrates specific binding to EGFR-expressing A431 cells. Competition experiments with other published anti-EGFR antibodies (P1X, P2X and mab806) reveal EGFR domain III as the target of C225, which agrees with published data[5-7]. EGFP fluorescence was measured in the FITC channel (see Methods section). Iso: isotype control. The experiment above was performed two times with similar results.

Supplementary Fig. 4: Site-directed biotinylation of Fc donor molecules and subsequent transfer to antibody acceptor modules

To enable site-directed biotinylation of binder-format matrices, Fc donor modules were generated that carry N-terminally fused Avi-tags for site-specific biotinylation via the BirA enzyme (see Methods section for details). These biotinylated donor Fc modules can be transferred to binder acceptor modules, resulting in defined biotinylated antibodies with intact antigen binding regions. These biotinylated antibody derivatives are defined reagents that can be used for assays such as SPR and immunoprecipitation. As an application example, immunoprecipitation of EGFR from total cell lysate using a biotinylated EGFR-binding pair-FORCE product is shown in Supplementary Fig. 4.

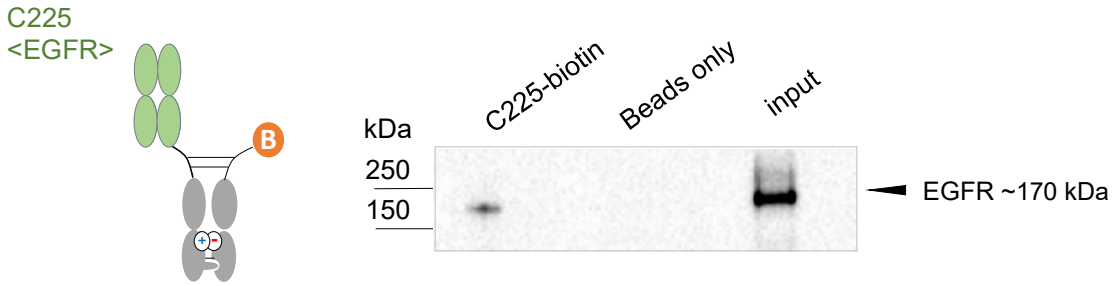

Supplementary Fig. 4: Transfer of site-specific biotinylated Fc donor module onto an EGFR-binding antibody derivative and application in an EGFR pull-down assay. Biotin was conjugated onto an Fc donor module via site-directed Avi-tag biotinylation using the enzyme BirA[8]. The functionality of the biotinylated antibody after chain-exchange with a C225 (Cetuximab) acceptor molecule was demonstrated by its application in immunoprecipitation of EGFR from A431 total cell lysate through immobilization of the biotinylated antibody onto magnetic streptavidin beads (see Methods section for details). Only the biotinylated C225 antibody was able to immunoprecipitate EGFR, whereas no EGFR was detected with streptavidin beads alone. The uncropped blot is provided at the end of the Supplementary Information section. The experiment above was performed one time.

Supplementary Fig. 5: Generation of Fc donor molecules for pair-FORCE: conjugation and quality control

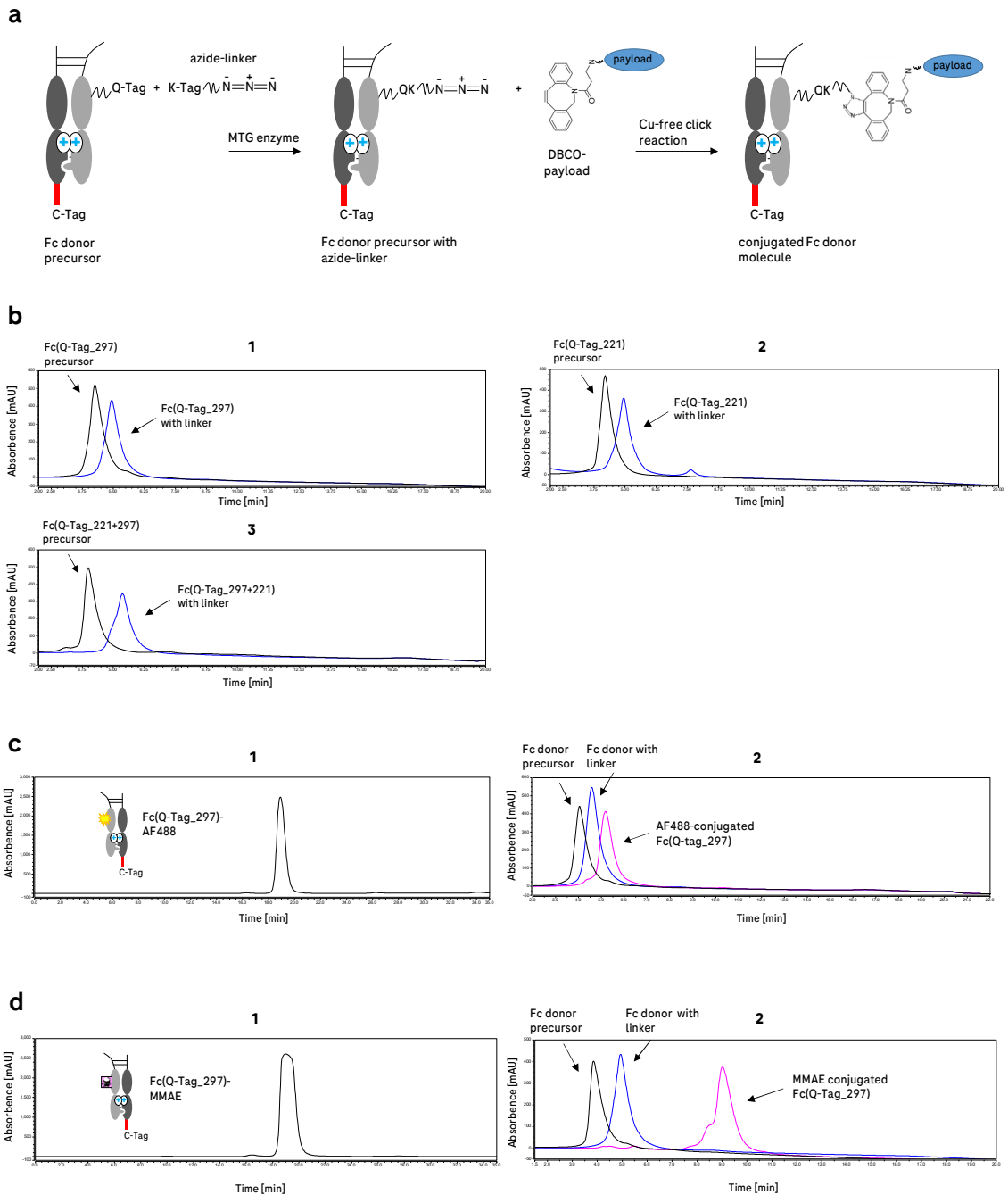

Supplementary Fig. 5: Payload conjugation onto Q-tags on Fc donor molecules with the two-step conjugation method. a Illustration of two-step conjugation with MTG-mediated azide conjugation followed by Cu-free click chemistry of a DBCO-payload moiety, as described in ref [9]. **b** Analytical HIC shows quantitative MTG-mediated azide-linker conjugation to Fc donors with (1) a Q-tag at position 297, (2) a Q-tag at position 221, and (3) Q-tags at positions 221+297. Fc donor-linker conjugates are more hydrophobic, which causes a longer retention time in HIC. **c** (1) SEC purification of an Fc donor

conjugated with AF488 using the two-step method. A SEC chromatogram after the Cu-free click reaction with AF488-DBCO is presented. (2) Analytical HIC of the AF488-DBCO two-step conjugation after the first and second steps. The HIC data shows quantitative MTG-mediated conjugation of the azide-linker and as well as quantitative AF488-DBCO conjugation via the Cu-free click reaction. **d** (1) SEC purification of an Fc donor conjugated with MMAE using the two-step method. A SEC chromatogram after the Cu-free click reaction with MMAE-DBCO is presented. (2) Analytical HIC of the MMAE-DBCO conjugation after the first and second steps. MMAE conjugation increases hydrophobicity of the Fc donor molecule, resulting in a longer retention time in HIC. The HIC data reveals quantitative MTG-mediated conjugation of the azide-linker as well as quantitative MMAE-DBCO conjugation via the Cu-free click reaction. Abbreviations: MTG: microbial transglutaminase, DBCO: Dibenzocyclooctyne, HIC: hydrophobic interaction chromatography, SEC: size exclusion chromatography, AF488: Alexa Fluor 488.

Supplementary Fig. 6: Exemplary intact ESI-MS spectra of MMAE-conjugated Fc donor molecules and Trastuzumab-derived, MMAE-conjugated pair-FORCE products

a

Fc(Q-tag_297)-MMAE

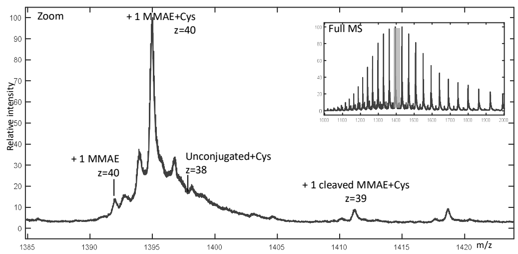

Intact ESI-MS after N-Deglycosylation with full scan and one selected zoom m/z area (grey)
Cys = Cysteinylation, unannotated signals are adducts, glycation or remaining glycosylation
Note: for DAR calculation, all labeled signals and all available charges were used. A cleaved MMAE was considered as unconjugated

b

Fc(Q-tag_221)-MMAE

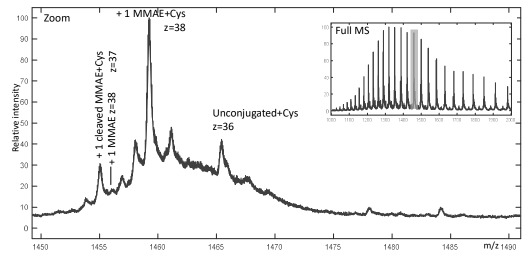

Intact ESI-MS after N-Deglycosylation with full scan and one selected zoom m/z area (grey)
Cys = Cysteinylation, unannotated signals are adducts, glycation or remaining glycosylation
Note: for DAR calculation, all labeled signals and all available charges were used. A cleaved MMAE was considered as unconjugated

c

Fc(Q-tag_297+221)-MMAE

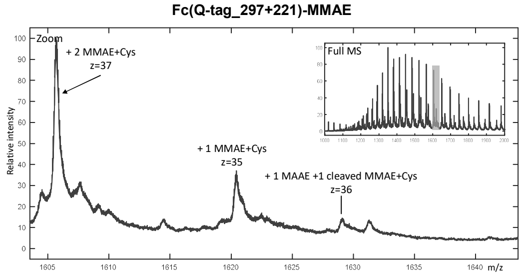

Intact ESI-MS after N-Deglycosylation with full scan and one selected zoom m/z area (grey)
Cys = Cysteinylation, unannotated signals are adducts, glycation or remaining glycosylation
Note: for DAR calculation, all labeled signals and all available charges were used. A cleaved MMAE was considered as unconjugated

d

Trastuzumab (N)_Fc(Q-tag_297)-MMAE

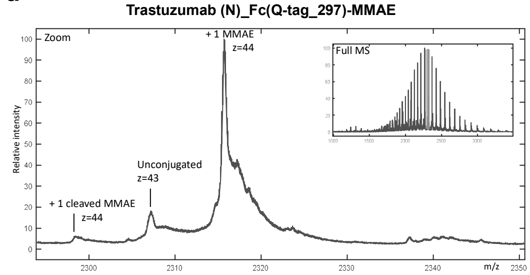

Intact ESI-MS after N-Deglycosylation with full scan and one selected zoom m/z area (grey)
Unannotated signals are adducts, glycation or remaining glycosylation
Note: for DAR calculation, all labeled signals and all available charges were used. A cleaved MMAE was considered as unconjugated

e

Trastuzumab (N)_Fc(Q-tag_221)-MMAE

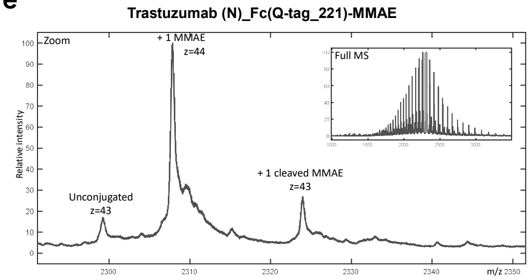

Intact ESI-MS after N-Deglycosylation with full scan and one selected zoom m/z area (grey)
Unannotated signals are adducts, glycation or remaining glycosylation
Note: for DAR calculation, all labeled signals and all available charges were used. A cleaved MMAE was considered as unconjugated

f

Trastuzumab (N)_Fc(Q-tag_297+221)-MMAE

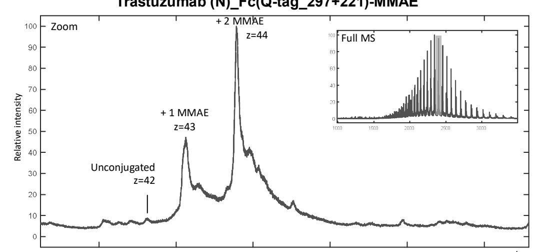

Intact ESI-MS after N-Deglycosylation with full scan and one selected zoom m/z area (grey)
Unannotated signals are adducts, glycation or remaining glycosylation
Note: for DAR calculation, all labeled signals and all available charges were used.

Supplementary Fig. 6: Exemplary intact ESI-MS spectra of MMAE-conjugated Fc donors and Trastuzumab pair-FORCE products for DAR determination. In order to calculate the DAR (drug-to-antibody ratio) of MMAE-conjugated antibody derivatives, intact ESI-MS (electrospray ionization-mass spectrometry) was performed after N-deglycosylation of the samples (see Methods section for details). For each spectrum, one selected zoom of m/z (mass-to-charge ratio) area is depicted, showing the peaks corresponding to MMAE-conjugated and unconjugated molecules, and molecules containing cleaved MMAE (deconjugated molecules). Shown above are exemplary ESI-MS spectra from one independent experiment (n=1), see Methods section for details. **a-c** Intact ESI-MS spectra of MMAE-conjugated Fc donors conjugated on positions 297, 221, or 221+297. **d-f** Intact ESI-MS spectra of Trastuzumab-derived pair-FORCE products in the N-format conjugated with MMAE at positions 297, 221, or 221+297.

Supplementary Fig. 7: Purity and integrity of MMAE-conjugated Fc donors, binder-acceptors, and pair-FORCE products

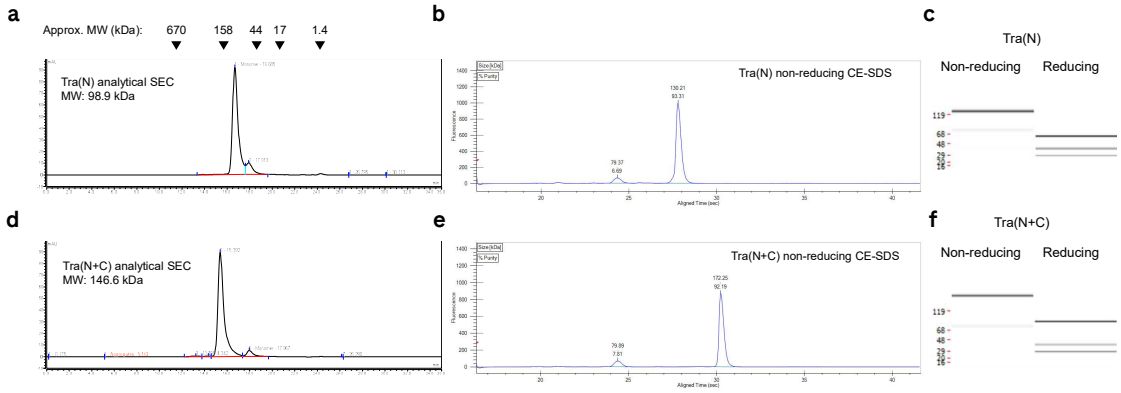

Table S7: Purity of pair-FORCE donors, acceptors, and products

Molecule	% Monomer	% Aggregates	% Purity in NR CE-SDS
Fc_Q-Tag(221)	91.7	0	99.0
Fc_Q-Tag(297)	92.8	0	97.3
Fc_Q-Tag(221+297)	93.6	0	95.9
FC_Q-Tag(221)+MMAE	*	0	98.3
FC_Q-Tag(297)+MMAE	*	0	98.0
FC_Q-Tag(221+297)+MMAE	*	0.3	95.4
Tra(N)	88.7	0	93.3
Tra(C)	94.4	0	95.1
Tra(N/C)	92.9	0	92.2
Per(N)	93.0	0	96.9
Per(C)	93.8	0	93.3
Per(N/C)	93.3	0	91.0
Tra(N)+Fc_Q-Tag(221)+MMAE	*	0	87.7
Tra(C)+Fc_Q-Tag(221)+MMAE	*	0	100
Tra(N+C)+Fc_Q-Tag(221)+MMAE	*	0	95.3
Per(N)+Fc_Q-Tag(221)+MMAE	*	0	90.8
Per(C)+Fc_Q-Tag(221)+MMAE	*	0	100
Per(N+C)+Fc_Q-Tag(221)+MMAE	*	0	94.7
Tra(N)+Fc_Q-Tag(297)+MMAE	*	0	93.2
Tra(C)+Fc_Q-Tag(297)+MMAE	*	0	96.0
Tra(N+C)+Fc_Q-Tag(297)+MMAE	*	0	93.1
Per(N)+Fc_Q-Tag(297)+MMAE	*	0	86.9
Per(C)+Fc_Q-Tag(297)+MMAE	*	0	94.1
Per(N+C)+Fc_Q-Tag(297)+MMAE	*	0	86.0
Tra(N)+Fc_Q-Tag(221+297)+MMAE	*	0	94.0
Tra(C)+Fc_Q-Tag(221+297)+MMAE	*	0	93.0
Tra(N+C)+Fc_Q-Tag(221+297)+MMAE	*	0.3	97.6
Per(N)+Fc_Q-Tag(221+297)+MMAE	*	0	90.9
Per(C)+Fc_Q-Tag(221+297)+MMAE	*	0.5	90.1
Per(N+C)+Fc_Q-Tag(221+297)+MMAE	*	0.5	100

Supplementary Fig. 7: Purity of MMAE-conjugated Fc donors, binder-acceptors, and pair-FORCE products used in the HER2 ADC screening matrix. Exemplary analytical SEC and CE-SDS chromatograms of HER2 pair-FORCE binder-acceptor molecules used in the HER2 ADC screening matrix. The analytical SEC and CE-SDS data is summarized in **Table S7** for all MMAE-conjugated Fc donors, Trastuzumab/Pertuzumab (Tra/Per) binder-acceptors, and MMAE-conjugated pair-FORCE products. **a** Analytical SEC chromatogram of the Trastuzumab (Tra) binder-acceptor molecule in the N-format. The monomer fraction corresponds to the larger peak. Approx. MW: approximate molecular weight in kilodalton. **b** Non-reducing CE-SDS electropherogram of the Trastuzumab (Tra) binder-

acceptor molecule in the N-format. **c** Virtual gel generated from non-reducing and reducing CE-SDS electropherograms of the Trastuzumab (Tra) binder-acceptor molecule in the N-format, showing the expected chain composition. Numbers on the left indicate the approximate MW in kDa. **d** Analytical SEC chromatogram of the Trastuzumab (Tra) binder-acceptor molecule in the N+C-format. The monomer fraction corresponds to the larger peak. **e** Non-reducing CE-SDS electropherogram of the Trastuzumab (Tra) binder-acceptor molecule in the N+C-format. **f** Virtual gel generated from non-reducing and reducing CE-SDS electropherograms of the Trastuzumab (Tra) binder-acceptor molecule in the N+C-format, showing the expected chain composition. Numbers on the left indicate the approximate MW in kDa. **Table S7:** *Monomer purity could not be calculated for MMAE-conjugated molecules due to interaction of the hydrophobic VC-PAB-MMAE compound with the column material, causing peak broadening and a shift in retention times.

Supplementary Fig. 8: Thermal stability of MMAE-conjugated Fc donors, binder-acceptors, and pair-FORCE products

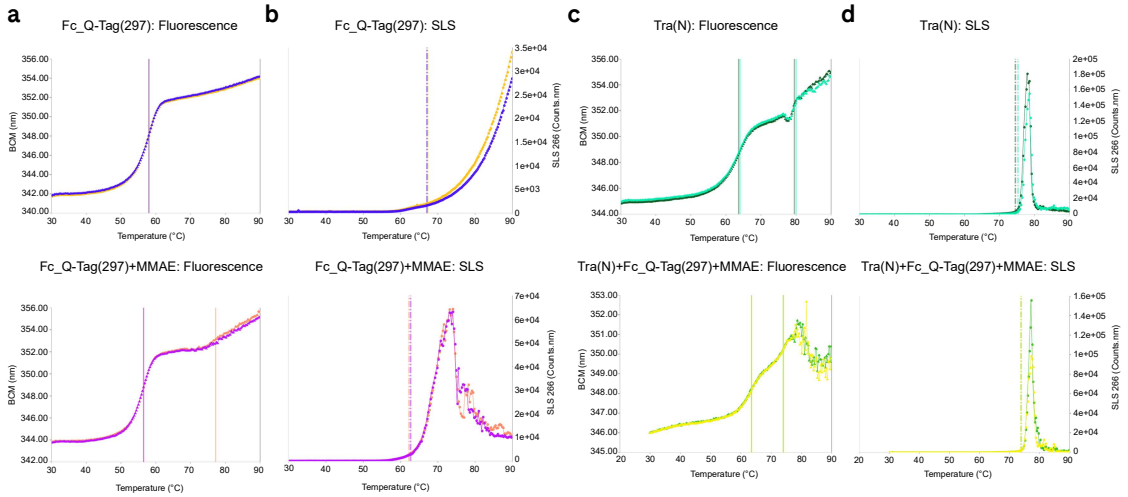

Table S8: Thermal stability of pair-FORCE donors, acceptors, and products

Molecule	Average T_m (°C)	SD T_m	Average T_{agg} (°C)	SD T_{agg}
Fc_Q-Tag(221)	60.6	0	73.9	0.3
Fc_Q-Tag(297)	58	0	67.2	0.1
Fc_Q-Tag(221+297)	58	0	59.9	0
FC_Q-Tag(221)+MMAE	59.5	0	67.6	0.1
FC_Q-Tag(297)+MMAE	56.5	0	62.5	0.2
FC_Q-Tag(221+297)+MMAE	54.6	0	54.3	0.2
Tra(N)	63.8	0.2	74.9	0.4
Tra(C)	64.5	0	75	0.1
Tra(N/C)	64.6	0.1	74.7	0.6
Per(N)	65.4	0.1	70.5	0
Per(C)	65.5	0	70.5	0
Per(N/C)	65.1	0.1	68.8	0.2
Tra(N)+Fc_Q-Tag(221)+MMAE	66	0	73	0.4
Tra(C)+Fc_Q-Tag(221)+MMAE	67.1	0.1	73.7	0.2
Tra(N+C)+Fc_Q-Tag(221)+MMAE	67.2	0	73.8	0
Per(N)+Fc_Q-Tag(221)+MMAE	71.5	0	70.6	0
Per(C)+Fc_Q-Tag(221)+MMAE	69.6	0.1	70.2	0
Per(N+C)+Fc_Q-Tag(221)+MMAE	70.5	0	69.5	0
Tra(N)+Fc_Q-Tag(297)+MMAE	63.5	0	73.9	0
Tra(C)+Fc_Q-Tag(297)+MMAE	61.1	0	73	0
Tra(N+C)+Fc_Q-Tag(297)+MMAE	63.3	0.2	73.1	0.1
Per(N)+Fc_Q-Tag(297)+MMAE	70.7	0	69.1	0
Per(C)+Fc_Q-Tag(297)+MMAE	69.8	0.3	69.6	0.1
Per(N+C)+Fc_Q-Tag(297)+MMAE	70.1	0.4	68.3	0.2
Tra(N)+Fc_Q-Tag(221+297)+MMAE	63.2	0	73.2	0.4
Tra(C)+Fc_Q-Tag(221+297)+MMAE	62.8	0.3	73	0
Tra(N+C)+Fc_Q-Tag(221+297)+MMAE	63	0	73.2	0
Per(N)+Fc_Q-Tag(221+297)+MMAE	71.3	0.3	69.4	0.2
Per(C)+Fc_Q-Tag(221+297)+MMAE	70.6	0.1	69.8	0
Per(N+C)+Fc_Q-Tag(221+297)+MMAE	70.1	0	69.3	0.2

Supplementary Fig. 8: Thermal stability of MMAE-conjugated Fc donors, binder-acceptors, and pair-FORCE products used in the HER2 ADC screening matrix. Exemplary thermal unfolding (nanoDSF) and aggregation spectra (SLS) of unconjugated and MMAE-conjugated Fc donors, HER2 binder acceptors, and MMAE-conjugated pair-FORCE products. In the nanoDSF spectra, the first inflection point was used to calculate the T_m. Abbreviations: NanoDSF: Nano differential scanning fluorimetry, SLS: static light scattering, BCM: barycentric mean, nm: nanometers. **Table S8** summarizes T_m (melting temperature) and T_{agg} (aggregation temperature) data for all molecules, derived

from spectra as shown in (**a-d**). Tra: Trastuzumab, Per: Pertuzumab. The data are presented as the mean and standard deviation (SD) from duplicate experiments (n=2). **a** Top: Thermal unfolding (nanoDSF) fluorescence spectrum of an Fc donor molecule with a Q-tag at position 297 (unconjugated). Bottom: NanoDSF fluorescence spectrum of an MMAE-conjugated Fc donor molecule at position 297. **b** Top: SLS spectrum of an Fc donor molecule with a Q-tag at position 297 (unconjugated). Bottom: SLS spectrum of an MMAE-conjugated Fc donor molecule at position 297. **c** Top: NanoDSF fluorescence spectrum of a Trastuzumab binder-acceptor molecule in the N-format. Bottom: NanoDSF fluorescence spectrum of a Trastuzumab pair-FORCE product in the N-format containing MMAE-conjugated at position 297. **d** Top: SLS spectrum of a Trastuzumab binder-acceptor molecule in the N-format. Bottom: SLS spectrum of a Trastuzumab pair-FORCE product in the N-format containing MMAE-conjugated at position 297.

Supplementary Fig. 9: Binding kinetics of HER2-targeting binder-acceptor molecules and MMAE-conjugated pair-FORCE products

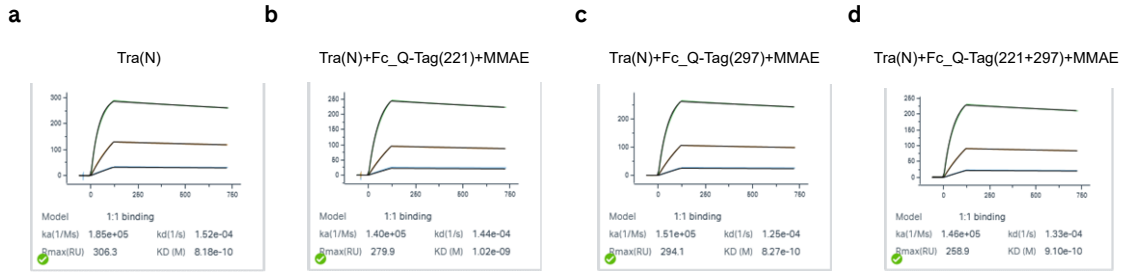

Table S9: Binding kinetics of HER2-targeting binder acceptors and pair-FORCE products

Sample	k_a (1/Ms)	k_d (1/s)	K_D (M)
Tra(N)	1.85E+05	1.52E-04	8.18E-10
Tra(C)	8.61E+04	1.75E-04	2.03E-09
Tra(N+C)	1.00E+05	9.19E-05	9.18E-10
Per(N)	1.30E+05	1.53E-04	1.18E-09
Per(C)	4.29E+04	1.92E-04	4.48E-09
Per(N+C)	8.43E+04	1.00E-04	1.19E-09
Tra(N)+Fc_Q-Tag(221)+MMAE	1.40E+05	1.44E-04	1.02E-09
Tra(C)+Fc_Q-Tag(221)+MMAE	9.52E+04	1.72E-04	1.80E-09
Tra(N+C)+Fc_Q-Tag(221)+MMAE	1.24E+05	1.05E-04	8.52E-10
Per(N)+Fc_Q-Tag(221)+MMAE	1.21E+05	1.48E-04	1.22E-09
Per(C)+Fc_Q-Tag(221)+MMAE	5.02E+04	1.42E-04	2.82E-09
Per(N+C)+Fc_Q-Tag(221)+MMAE	8.56E+04	9.77E-05	1.14E-09
Tra(N)+Fc_Q-Tag(297)+MMAE	1.51E+05	1.25E-04	8.27E-10
Tra(C)+Fc_Q-Tag(297)+MMAE	1.04E+05	1.18E-04	1.14E-09
Tra(N+C)+Fc_Q-Tag(297)+MMAE	9.50E+04	9.57E-05	1.01E-09
Per(N)+Fc_Q-Tag(297)+MMAE	1.30E+05	1.36E-04	1.05E-09
Per(C)+Fc_Q-Tag(297)+MMAE	6.58E+04	1.45E-04	2.20E-09
Per(N+C)+Fc_Q-Tag(297)+MMAE	8.25E+04	9.03E-05	1.09E-09
Tra(N)+Fc_Q-Tag(221+297)+MMAE	1.46E+05	1.33E-04	9.10E-10
Tra(C)+Fc_Q-Tag(221+297)+MMAE	1.07E+05	1.07E-04	9.98E-10
Tra(N+C)+Fc_Q-Tag(221+297)+MMAE	9.97E+04	8.05E-05	8.07E-10
Per(N)+Fc_Q-Tag(221+297)+MMAE	1.22E+05	1.56E-04	1.28E-09
Per(C)+Fc_Q-Tag(221+297)+MMAE	5.98E+04	1.13E-04	1.90E-09
Per(N+C)+Fc_Q-Tag(221+297)+MMAE	8.68E+04	8.62E-05	9.93E-10

Supplementary Fig. 9: Binding kinetics of HER2-targeting binder-acceptors and MMAE-conjugated pair-FORCE products to HER2. To investigate the influence of pair-FORCE using MMAE-conjugated Fc donors on HER2 binding kinetics, SPR (surface plasmon resonance) assays were performed. HER2-targeting binder-acceptor molecules and MMAE-conjugated HER2-targeting pair-FORCE products were immobilized onto SPR chips, and HER2-Fc antigen was flowed as the analyte (see Methods section for details). The data shows that HER2 binding kinetics of binder-acceptor precursors are overall very similar to the HER2-MMAE pair-FORCE products. **a-d** Exemplary SPR sensorgrams are depicted (n=1 independent experiment). The fitted curves in blue, brown, and green correspond to HER2-Fc antigen concentrations of 5 nM, 25 nM, and 125 nM, respectively. The binding kinetics for all molecules are summarized in **Table S9**. **a** SPR sensorgrams of a Trastuzumab-derived binder-acceptor molecule in the N-format. **b** SPR sensorgrams of a Trastuzumab-derived pair-FORCE product in the N-format conjugated with MMAE on position 221. **c** SPR sensorgrams of a Trastuzumab-derived pair-FORCE product in the N-format conjugated with MMAE on position 297. **d** SPR sensorgrams of a Trastuzumab-derived pair-FORCE product in the N-format conjugated with MMAE on positions 221+297. Abbreviations: Tra: Trastuzumab, Per: Pertuzumab, k_a: association constant, k_d:

dissociation constant, K_D: equilibrium constant. The format of each construct is indicated in brackets (N, C, and N/C correspond to the formats shown in **Fig. 1b** of the main text).

Supplementary Fig. 10: Cytotoxic activity of pair-FORCE-generated MMAE ADCs on target-overexpressing cell lines

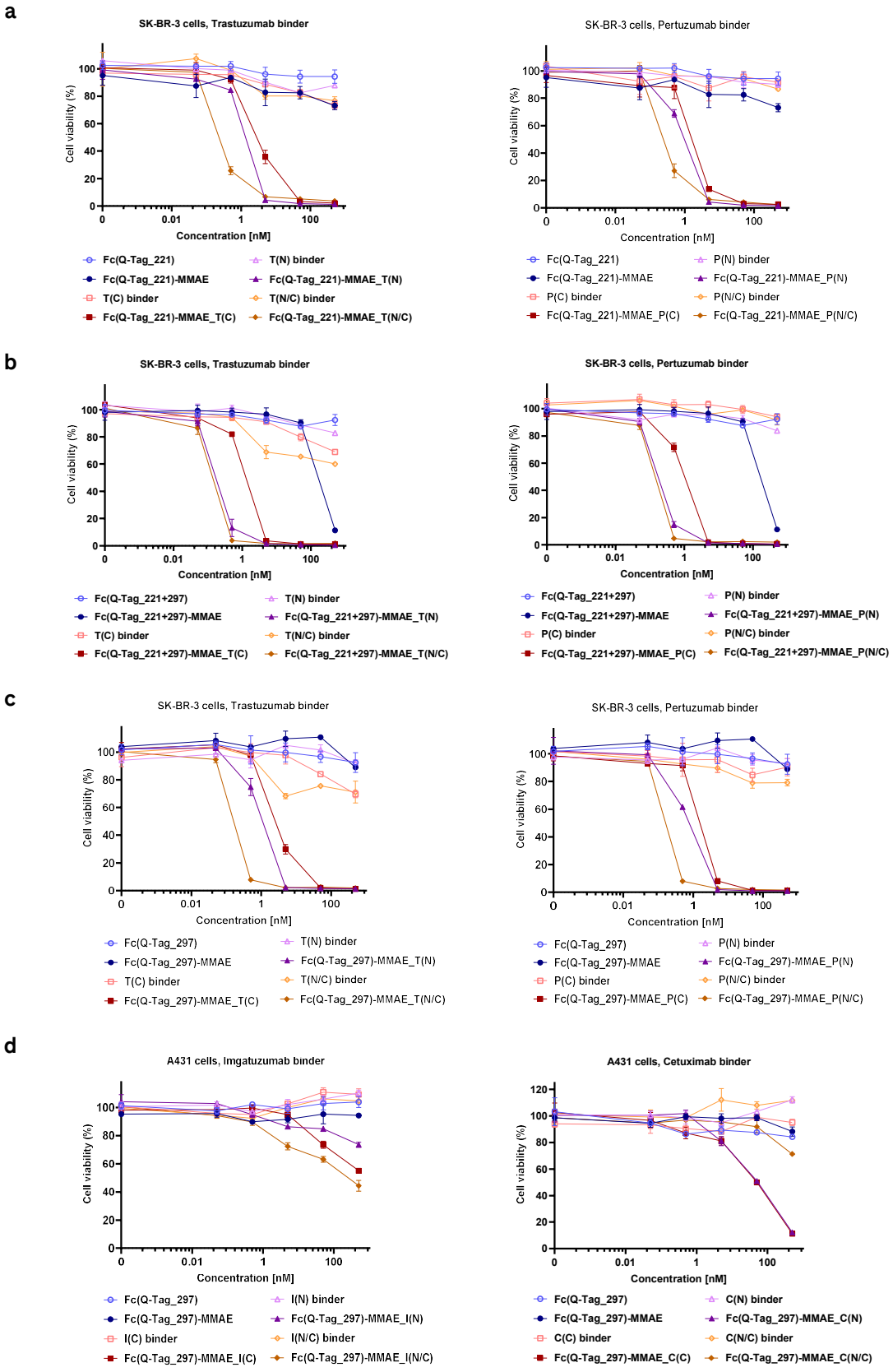

Supplementary Fig. 10: Activity of pair-FORCE-generated, MMAE-containing ADCs on target-overexpressing cell lines. Cell viability was measured by incorporation of BrdU (bromodeoxyuridine) upon treatment with respective antibody derivatives (see Methods section for details). SK-BR-3 and A431 cells express high levels of HER2 and EGFR, respectively[10]. Abbreviations are as follows: T: Trastuzmab, P: Pertuzumab, I: Imgatuzumab, C: Cetuximab. The format of each construct is indicated in brackets (N, C, and N/C correspond to the formats shown in **Fig. 1b** of the main text). All data are presented as the mean and standard deviation from triplicate experiments (n=3). **a** HER2-expressing SK-BR-3 cells were treated for 72 h with Trastuzmab-derived antibody derivatives containing MMAE conjugated to a Q-tag on position 221 (left panel). The same assay with MMAE-conjugated Pertuzumab-derived binders is shown in the right panel. **b** HER2-expressing SK-BR-3 cells were treated for 72 h with Trastuzmab-derived antibody derivatives containing MMAE conjugated to Q-tags on positions 221+297 (left panel). The same assay with Pertuzumab-derived binders containing MMAE on Q-tags at positions 221+297 is shown in the right panel. **c** HER2-expressing SK-BR-3 cells were treated for 72 h with Trastuzumab-derived antibody derivatives containing MMAE conjugated to a Q-tag on position 297 (left panel). An assay with Pertuzumab-derived antibody derivatives containing MMAE conjugated to a Q-tag on position 297 is shown in the right panel. **d** EGFR-expressing A431 cells were treated for 72 h with Imgatuzumab-derived antibody derivatives containing MMAE conjugated to a Q-tag on position 297 (left panel). In the panel on the right, the same assay with Cetuximab-derived antibody derivatives containing MMAE conjugated to a Q-tag on position 297 is shown. Source data are provided as a Source Data file.

Supplementary Fig. 11: Cytotoxic activity of HER2-MMAE and EGFR-MMAE ADCs on cells expressing low levels of target antigen

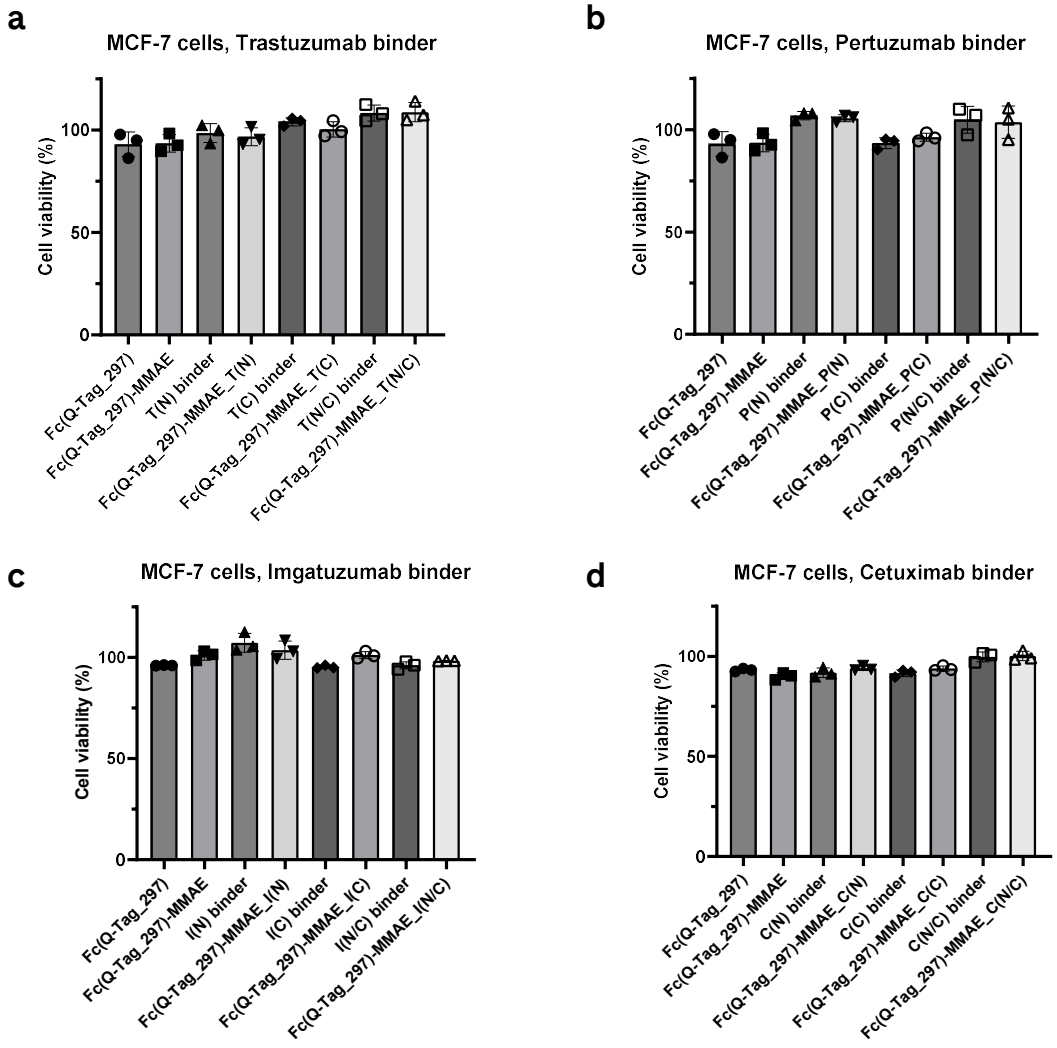

Supplementary Fig. 11: Activity of pair-FORCE-generated, MMAE-containing HER2 and EGFR ADCs on a low-HER2/EGFR-expressing cell line. Viability of MCF-7 cells was measured by BrdU (bromodeoxyuridine) incorporation at an ADC concentration of 50 nM. MCF-7 cells express low levels of HER2 and EGFR[10]. Abbreviations are as follows: T: Trastuzmab, P: Pertuzumab, I: Imgatuzumab, C: Cetuximab. The format of each construct is indicated in brackets (N, C, and N/C correspond to the formats shown in **Fig. 1b** of the main text). All ADCs tested above contain a Q-tag on position 297 and were generated by pair-FORCE. All tested ADCs are inactive on MCF-7 cells, indicating that target overexpression is a requirement for HER2 and EGFR ADC cytotoxicity in the above formats. The data are presented as the mean and standard deviation from triplicate experiments (n=3). **a** Cytotoxicity of Trastuzumab-derived HER2-MMAE ADCs on MCF-7 cells. **b** Cytotoxicity of Pertuzumab-derived HER2-MMAE ADCs on MCF-7 cells. **c** Cytotoxicity of Imgatuzumab-derived EGFR-MMAE ADCs on MCF-7 cells. **d** Cytotoxicity of Cetuximab-derived EGFR-MMAE ADCs on MCF-7 cells. Source data are provided as a Source Data file.

Supplementary Fig. 12: Cytotoxic activity of HER2-MMAE ADCs on cell lines expressing different levels of HER2

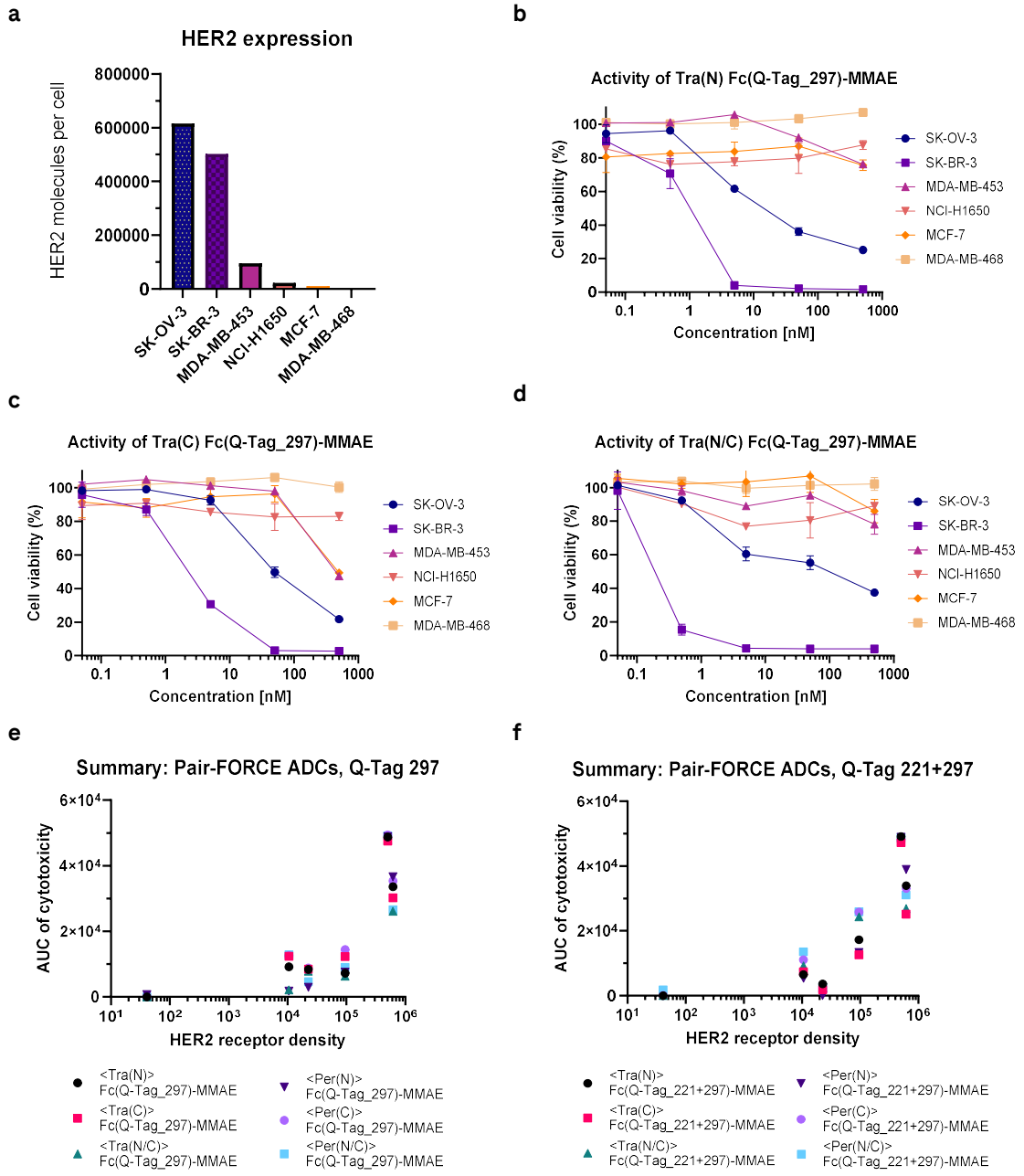

Supplementary Fig. 12: Cytotoxic activity of HER2-MMAE ADCs on cell lines expressing different levels of HER2. a The number of HER2 receptors per cell was quantified for various cell lines using the QIFIKIT quantitative analysis kit (Agilent K0078, see Methods section for details), n=1 independent experiment. **b-d** The cytotoxic activity of the indicated pair-FORCE-generated HER2-MMAE ADCs was tested on cell lines expressing different levels of HER2, as in **Supplementary Fig. 10**. The data are presented as the mean and standard deviation from duplicate experiments (n=2). **e** The cytotoxic activity of the indicated Trastuzumab (Tra) or Pertuzumab (Per) ADCs with MMAE conjugated on position 297 was plotted as a function of HER2 receptor density. Cytotoxicity was calculated from dose-response curves as in (**b-d**) using the area under curve approach (AUC). **f** The cytotoxic activity of the indicated Trastuzumab (Tra) or Pertuzumab (Per) ADCs with MMAE conjugated on positions 221+297 was plotted as a function of HER2 receptor density, as in (**e**). The

format of each construct is indicated in brackets (N, C, and N/C correspond to the formats shown in **Fig. 1b** of the main text). Source data are provided as a Source Data file.

Supplementary References

1. Ridgway, J.B., Presta, L.G. & Carter, P. 'Knobs-into-holes' engineering of antibody CH3 domains for heavy chain heterodimerization. *Protein Eng* **9**, 617-621 (1996).

2. Dengl, S. et al. Format chain exchange (FORCE) for high-throughput generation of bispecific antibodies in combinatorial binder-format matrices. *Nat Commun* **11**, 4974 (2020).

3. Goldstein, N.I., Prewett, M., Zuklys, K., Rockwell, P. & Mendelsohn, J. Biological efficacy of a chimeric antibody to the epidermal growth factor receptor in a human tumor xenograft model. *Clin Cancer Res* **1**, 1311-1318 (1995).

4. Abdiche, Y.N., Lindquist, K.C., Stone, D.M., Rajpal, A. & Pons, J. Label-free epitope binning assays of monoclonal antibodies enable the identification of antigen heterogeneity. *Journal of immunological methods* **382**, 101-116 (2012).

5. Li, S. et al. Structural basis for inhibition of the epidermal growth factor receptor by cetuximab. *Cancer Cell* **7**, 301-311 (2005).

6. Kearns, J.D. et al. Enhanced Targeting of the EGFR Network with MM-151, an Oligoclonal Anti-EGFR Antibody Therapeutic. *Mol Cancer Ther* **14**, 1625-1636 (2015).

7. Johns, T.G. et al. Identification of the epitope for the epidermal growth factor receptor-specific monoclonal antibody 806 reveals that it preferentially recognizes an untethered form of the receptor. *The Journal of biological chemistry* **279**, 30375-30384 (2004).

8. Beckett, D., Kovaleva, E. & Schatz, P.J. A minimal peptide substrate in biotin holoenzyme synthetase-catalyzed biotinylation. *Protein Sci* **8**, 921-929 (1999).

9. Sela, T. et al. Diligent Design Enables Antibody-ASO Conjugates with Optimal Pharmacokinetic Properties. *Bioconjug Chem* **34**, 2096-2111 (2023).

10. Smith, S.E. et al. Molecular characterization of breast cancer cell lines through multiple omic approaches. *Breast Cancer Res* **19**, 65 (2017).

Uncropped gels and blots:

Fig. 2a:

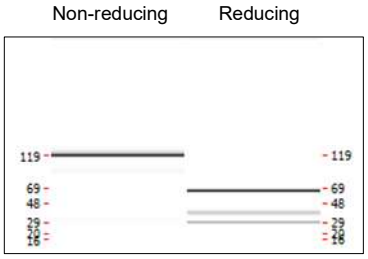

Supplementary Fig. 1b:

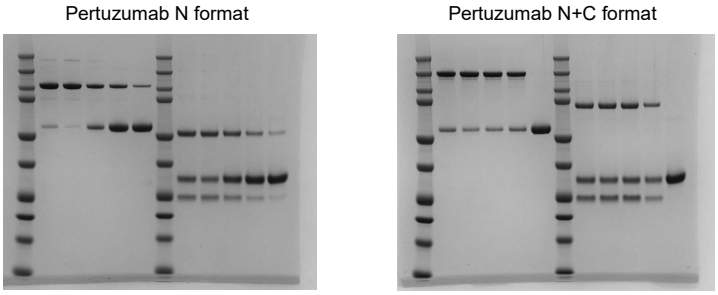

Supplementary Fig. 1e:

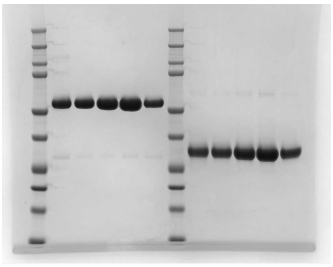

Supplementary Fig. 2:

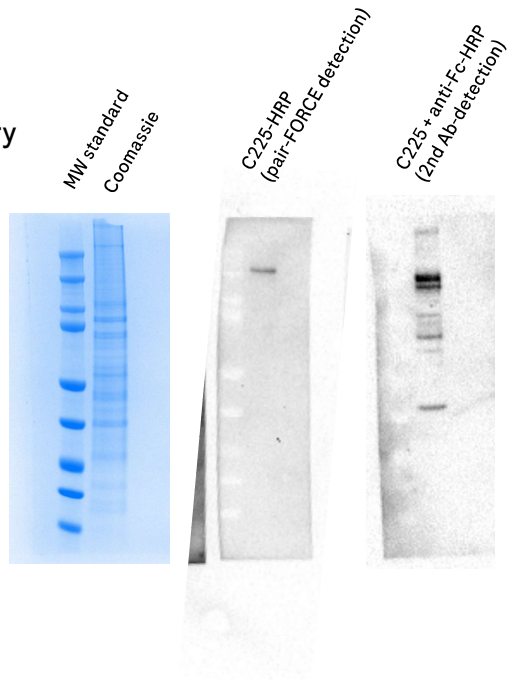

Supplementary Fig. 4:

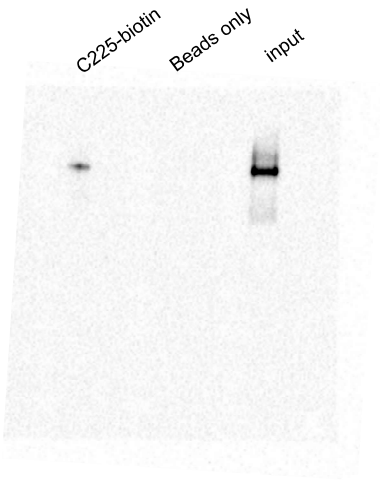

Gating strategy for flow cytometry experiments:

Fig. 3:

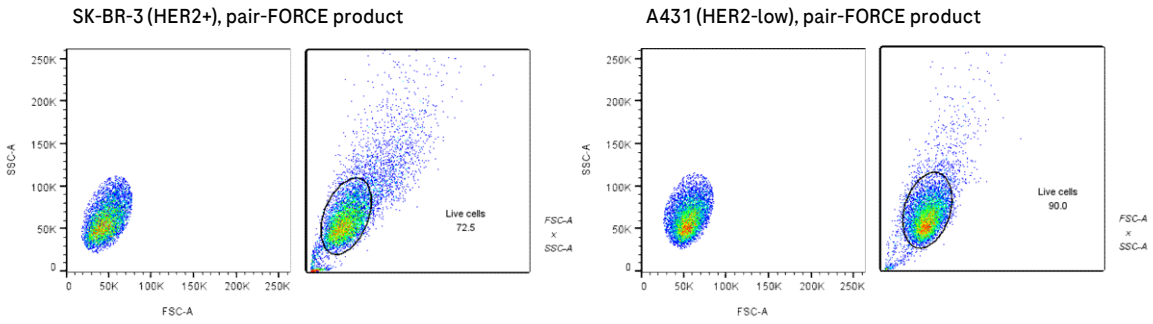

Fig. 4:

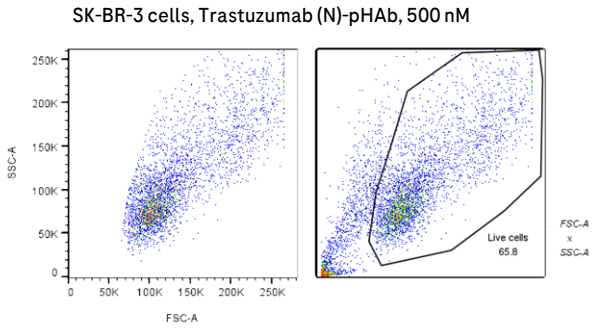

Supplementary Fig. 3: